LAWRENCE
LIVERMORE
NATIONAL
LABORATORY

UCRL-JRNL-207513

Propagation of Weakly Guided Waves in a Kerr Nonlinear Medium using a Perturbation Approach

Jennifer Dacles-Mariani, Garry Rodrigue

October 27, 2004

Communications in Nonlinear Science and Numerical Simulation

Disclaimer

Propagation of weakly guided waves in a Kerr nonlinear medium using a perturbation approach ⋆

Jennifer Dacles-Mariani *,1 Garry Rodrigue [1]

Department of Applied Science
University of California Davis, CA 95616

Abstract

The equations are represented in a simplified format with only a few leading terms needed in the expansion. The set of equations are then solved numerically using vector finite element method. To validate our algorithm, we analyzed a two-dimensional rectangular waveguide consisting of a linear core and nonlinear identical cladding. The exact nonlinear solutions for three different modes of propagations, TE0, TE1, and TE2 modes are generated and compared with the computed solutions. Next, we investigate the effect of a more intense monochromatic field on the propagation of a "weak" optical field in a fully three-dimensional cylindrical waveguide.

Key words: Kerr effect, Maxwell's equations, optical fiber, vector finite element
PACS: 84.40.Az, 83.20.Wt

1 Introduction

Changes in the refractive index of a material can be induced by the application of an external electric field. The presence of such a field distorts the

⋆ This work was performed under the auspices of the U.S. Department of Energy by the University of California, Lawrence Livermore National Laboratory under contract No. W-7405-Eng-48,and under the U.S. AFOSR Contract No. F49620-01-0327. UCRL-JRNL-207513

* Tel.(925)422-4032, Fax(925)422-7819
Email addresses: daclesmariani1@llnl.gov (Jennifer Dacles-Mariani), ghrodrigue@ucdavis.edu (Garry Rodrigue).
[1] University of California, Davis and Institute for Scientific Computing Research, Lawrence Livermore National Laboratory

electron motions in the atoms or molecules of a substance, or distorts the crystal structure so that changes in the optical properties occur.This physical phenomenon is known as Kerr effect. The refractive index in this case is expressed as $n_0 + \alpha|E|^2$, where the total refractive index consists of the linear refractive index n_0 and an added effect due to the intensity of an externally applied field with α as the Kerr coefficient of the material. Non-linear Kerr effects in optical fibers are manifested in such effects as optical solitons, pulse compressions and modulation instabilities. Although the nonlinearity of silica-based optical fibers are small, some nonlinear effects can be observed without difficulty.

We begin with the second-order wave equation governing the propagation of light in a nonlinear medium as derived from Maxwell's equations for an arbitrary homogeneous dielectric medium as

$$\nabla^2\mathbf{E} - \frac{1}{c^2}\frac{\partial^2\mathbf{E}}{\partial t^2} = \frac{4\pi}{c^2}\frac{\partial^2\mathbf{P}}{\partial t^2} \tag{1}$$

where c is the speed of light in vacuum, and $\mathbf{P} = \Psi(\mathbf{E})$ is a nonlinear function of the electric field $\mathbf{E}$, at every position in time. We write $\mathbf{P}$ as a sum of linear and nonlinear parts

$$\mathbf{P} = \chi^{(1)}\mathbf{E} + \mathbf{P}_{NL} \tag{2}$$

where

$$\mathbf{P}_{NL} = \chi^{(2)}\mathbf{E}^2 + \chi^{(3)}\mathbf{E}^3 + h.o.t. \tag{3}$$

It follows from Eqn. 1 that

$$\nabla^2\mathbf{E} - \frac{\epsilon_0}{c^2}\frac{\partial^2\mathbf{E}}{\partial t^2} = \frac{4\pi}{c^2}\frac{\partial^2\mathbf{P}}{\partial t^2} \tag{4}$$

where $\epsilon_0 = 1+4\pi\chi^{(1)}$. In a media possessing centrosymmetry, the second-order nonlinear term is absent since the polarization must reverse exactly when the electric field is reversed. The dominant nonlinearity is then of third order,

$$\mathbf{P}_{NL} = \chi^{(3)}\mathbf{E}^3 \tag{5}$$

where $\chi^{(3)}$ is a third-order tensor. These equations provide the general framework for studying third-order nonlinear effect which is also known as optical Kerr effect. In addition, if we assume an electric field, $\mathbf{E}(\mathbf{t})$, of the form

$$\mathbf{E}(t) = \mathbf{E}(\omega)e^{i\omega t} \tag{6}$$

it then follows that for a linearly polarized field, we get $\mathbf{E}(\omega) = \hat{x}\chi^{(3)}_{1111}|\mathbf{E}(\omega)|^2 E(\omega)$. Consequently, the wave equation governing the propagation of light in a non-linear medum can often be represented by

$$\nabla^2\mathbf{E} - (n_0 + \alpha|\mathbf{E}|^2)\frac{\partial^2\mathbf{E}}{\partial t^2} = 0 \tag{7}$$

where $n_0 = \epsilon_0/c^2$ and $\alpha = (4\pi\tilde{\chi})/c^2$. Typically, changes in the refractive index by Kerr effects are small and values for $\tilde{\chi}$ are in the range of $10^{-10} - 10^{-13}$.

2 Perturbation Method Applied to Non-linear Maxwells Equation

In the case where the governing equations are nonlinear, one approach is to use a perturbation series solution to analyze the behavior of the function in a limiting situation. We consider the numerical solution of the nonlinear wave equation given by

$$\nabla^2\mathbf{E} - (n_0 + \alpha|\mathbf{E}^2|)\frac{\partial^2\mathbf{E}}{\partial t^2} = 0. \tag{8}$$

The approach is to try a power series solution such as

$$\mathbf{E}(\mathbf{x}, t) = \mathbf{E}_0(\mathbf{x}, t) + \alpha\mathbf{E}_1(\mathbf{x}, t) + \alpha^2\mathbf{E}_2(\mathbf{x}, t) + h.o.t. \tag{9}$$

The series is inserted into Eqn. 8, along with the corresponding boundary conditions.Then the coefficients with like powers are grouped together. We then get

$$\nabla^2\mathbf{E}_0 - n_0\frac{\partial^2\mathbf{E}_0}{\partial t^2} = 0 \tag{10}$$

$$\nabla^2\mathbf{E}_1 - n_0\frac{\partial^2\mathbf{E}_1}{\partial t^2} = |\mathbf{E}_0|^2\frac{\partial^2\mathbf{E}_0}{\partial t^2} = n_0^{-1}|\mathbf{E}_0|^2\nabla^2\mathbf{E}_0 \tag{11}$$

and so on. In doing so, the problem of solving the nonlinear wave equation (Eqn. 8), can be done by solving the two linear wave equations Eqns. 10 and 11, over a time interval and adding the two solutions to get

$$\mathbf{E} = \mathbf{E}_0(\mathbf{x}, t) + \alpha\mathbf{E}_1(\mathbf{x}, t) \tag{12}$$

Note that the resulting series does not need to to converge for any value of α. For most practical applications, the solution is useful in approximating the

equation even with just two or three terms on the expansion. From a computational standpoint convergence of the series refers to the behavior of the equation towards the tail end of the series. In an asymptotic series, the terms decrease rapidly for sufficiently small α. When the terms decrease rapidly, if we sum just the few terms, we know that the error incurred is of the order of the next term; which means that we can get a good estimate of the sum. This is one reason why asymptotic series, even when divergent, are pratically useful. In our study, we validate the perturbation approach by comparison with known analytical solution for a two-dimensional weakly guided optical wave propagating a three-layer optical guide with a linear core and a nonlinear cladding.

3 Vector Finite Element Formulation

Numerical solutions of the linear wave equations are first obtained by first converting the linear wave equations into a variational equation posed over suitable function spaces. We denote $L_2(\Omega)$ to be a Hilbert space of functions with $|\mathbf{u}|_2^2 \equiv \int_\Omega \mathbf{u}^T\mathbf{u}\ d(\Omega) < \infty$ and inner product $(\mathbf{u},\mathbf{v}) = \int_\Omega \mathbf{u}^T\mathbf{v}\ d(\Omega)$. The Hilbert space

$$\mathbf{H}(curl;\Omega) = \{\mathbf{u} \in \mathbf{L}_2(\Omega) : \nabla\times\mathbf{u} \in \mathbf{L}_2(\Omega)\} \tag{13}$$

If K_1 and K_2 are two domains that border on one another, then $\mathbf{u} \in \mathbf{H}(curl;\Omega = \mathbf{K}_1 \cup \mathbf{K}_2)$ if and only if $\mathbf{u}\times\mathbf{n}$ is the same on each side of the face $\Gamma = \mathbf{K}_1 \cap \mathbf{K}_2$ [1]. As usual, $\mathbf{n}$ is designated the exterior unit normal on Γ. Consequently, $\mathbf{H}(curl;\Omega)$ is an appropriate space for the electric field $\mathbf{E}$. The subspace of $\mathbf{H}(curl;\Omega)$ containing the vector fields wiith vanishing tangential trace $\mathbf{u}\times\mathbf{n}$ on Γ = Boundary (Ω) is denoted by $\mathbf{H}_0(curl;\Omega)$.

A natural way of defining the weak form of the linear wave equation (Eq.10), is to determine a function $\mathbf{E}_0 \in \mathbf{H}(curl;(\Omega)$ such that

$$\frac{\partial^2}{\partial t^2}(n_0\mathbf{E}_0, \mathbf{E}^*) = (\nabla^2\mathbf{E}_0, \nabla\mathbf{E}^*) \tag{14}$$

for all $\mathbf{E}^* \in \mathbf{H}(curl;\Omega)$. Consequently, if $\mathbf{E}_0$ is a classical solution of the nonlinear wave equation, then it is a solution of the weak equation.

We shall approximate the domain Ω with a hexahedral mesh consisting of $\mathbf{K}_1, i = 1, ..., N$ hexahedra. Each of the hexahedra K can be mapped using the standard one-to-one trilinear mapping $(x, y, z) = B(\xi, \eta, \psi)$ to the reference

element $\mathbf{K}_0 = \{-1 \leq \Psi, \eta, \zeta \leq 1\}$, see Figure 1. This implies that the mapping B has a nonsingular Jacobian matrix J.

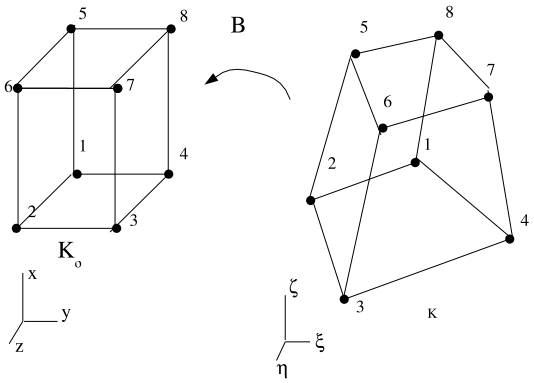

Fig. 1. Reference element $K_0 = \{-1 \leq \Psi, \eta, \zeta \leq 1\}$.

The edge labeling convention consistent with the node labeling for the hexahedra is tabulated below.

i	$edge, \tilde{a}_i$	i	$edge, \tilde{a}_i$
1	1-2	7	2-3
2	4-3	8	6-7
3	5-6	9	1-5
4	8-7	10	2-6
5	1-4	11	4-8
6	5-8	12	3-7

Next, we define vector polynomials on K_0 as follows

$$\begin{aligned}
&\mathbf{W}_1^{(0)} = [(1-y)(1-z) \;\; 0 \;\; 0] \quad \mathbf{W}_3^0 = [0 \;\; (1-x)(1-z) \;\; 0] \quad \mathbf{W}_9^{(0)} = [0 \;\; 0 \;\; (1-x)(1-y)] \\
&\mathbf{W}_2^{(0)} = \tfrac{1}{2}[(y+1)(1-z) \;\; 0 \;\; 0] \; \mathbf{W}_6^0 = \tfrac{1}{2}[0 \;\; (x+1)(1-z) \;\; 0] \; \mathbf{W}_1^{(0)}0 = \tfrac{1}{2}[0 \;\; 0 \;\; (x+1)(1-y)] \\
&\mathbf{W}_3^{(0)} = \tfrac{1}{2}[(z+1)(1-y) \;\; 0 \;\; 0] \; \mathbf{W}_7^0 = \tfrac{1}{2}[0 \;\; (z+1)(1-x) \;\; 0] \; \mathbf{W}_9^{(0)} = \tfrac{1}{2}[0 \;\; 0 \;\; (y+1)(1-x)] \\
&\mathbf{W}_4^{(0)} = \tfrac{1}{4}[(y+1)(z+1) \;\; 0 \;\; 0] \; \mathbf{W}_8^0 = \tfrac{1}{4}[0 \;\; (x+1)(z+1) \;\; 0] \; \mathbf{W}_9^{(0)} = \tfrac{1}{4}[0 \;\; 0 \;\; (x+1)(y+1)]
\end{aligned} \tag{15}$$

Note that $\oint\limits_{\alpha_i} W_j^{(0)} = \delta_{ij}$. Vector polynomials on K are given by $W_i = J_{-1} W_i^{(0)}$.

The Galerkin method shown below[2], constructs approximations

$$\tilde{\mathbf{E}}_\mathbf{0} = \sum_{i=1}^{n_e} e_j W_j \in span[W_1, ..., W_N] \subset H_0(curl : \Omega) \tag{16}$$

such that

$$\frac{\partial^2}{\partial t^2}(n_1\tilde{\mathbf{E}}_0, \mathbf{W}_i) = (\nabla\tilde{\mathbf{E}}_0, \nabla\mathbf{W}_i), i = 1, ..., N_e \tag{17}$$

where N_e is the number of internal edges. This results in a set of ordinary differential equations

$$\mathbf{M}\frac{d^2\mathbf{e}_0}{dt^2} = \mathbf{K}\mathbf{e}_0 \tag{18}$$

where

$$\mathbf{M} = n_1\mathbf{matrix}[(\mathbf{W_i}, \mathbf{W_j})] \quad \mathbf{K} = \mathbf{matrix}[(\nabla\mathbf{W_i}, \nabla\mathbf{W_j})] \tag{19}$$

Leap-frog time differencing is used to integrate Eqn. 18;

$$\begin{bmatrix} \mathbf{e}_0^{n+1} \\ \mathbf{e}_0^n \end{bmatrix} = \begin{bmatrix} 2\mathbf{M} + \Delta t^2\mathbf{K} & -\mathbf{I} \\ \mathbf{I} & \mathbf{0} \end{bmatrix} \begin{bmatrix} \mathbf{e}_0^n \\ \mathbf{e}_0^{n-1} \end{bmatrix} \tag{20}$$

A similar discretization of Eqn. 11 yields the set of ordinary differential equations

$$\mathbf{M}\frac{d^2\mathbf{e}_1}{dt^2} = \mathbf{K}\mathbf{e}_1 + n_1^{-1}|\mathbf{e}_0|^2\mathbf{K}\mathbf{e}_0 \tag{21}$$

Leap-frog time differencing of Eqn. 21 yields

$$\begin{bmatrix} \mathbf{e}_1^{n+1} \\ \mathbf{e}_1^n \end{bmatrix} = \begin{bmatrix} 2\mathbf{M} + \Delta t^2\mathbf{K} & -\mathbf{I} \\ \mathbf{I} & \mathbf{0} \end{bmatrix} \begin{bmatrix} \mathbf{e}_1^0 \\ \mathbf{e}_1^{n-1} \end{bmatrix} + n_1^{-1}\Delta t^2|\mathbf{e}_0^{n+1}|^2 \begin{bmatrix} \mathbf{e}_0^{n+1} \\ 0 \end{bmatrix} \tag{22}$$

The numerical solution is then given by

$$\mathbf{e}^{n+1} = \mathbf{e}_0^{n+1} + \alpha\mathbf{e}_1^{n+1}. \tag{23}$$

4 Numerical Solution of the Non-Linear Wave Equation

In general, nonlinear solutions can't be solved exactly except for certain nonlinear wave equations. The exact solutions for stationary and unbounded Kerr nonlinear medium[3] are adopted here as our starting point in validating our

approach. We first consider the exact solution of the nonlinear wave equation where we assume the solution to be of the form

$$\mathbf{E}(\mathbf{x},t) = \begin{bmatrix} 0 \\ E_y \\ 0 \end{bmatrix} \exp^{i\beta z - i\omega t} \tag{24}$$

The geometry is shown below in Fig. 2. It has the linear core sandwiched by two identical nonlinear cladding. We consider three modes; TE0, TE1 and TE2 modes. TE0 mode is an optical wave with a maximum located in the core region and decays monotonically in the cladding. TE1 mode has two field maxima and depending on the intensity of the applied field, it can have the maxima inside the core or in the cladding. Finally, the TE2 mode has 3 field maxima, one inside the core and the other two in the cladding. The modes that have the field maxima in the nonlinear cladding is especially important [4],[5], since these are responsible for the optically controlled directional couplers.

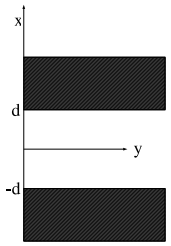

Fig. 2. Geometry of a three-layer optical guide with a linear core and nonlinear cladding.

In our validation study, we used the equations given below and extended the geometry in the cladding such that far-field approximations can be used and will not interfere with the actual cladding solution. Time dependence is also included in both the exact and computed solutions.

The general solutions for each layer are

$$E_y^{(0)}(x) = Asech[-\gamma(x-d)+\psi_0] \quad x \geq d \tag{25}$$

$$E_y^{(1)}(x) = Bcos[K(x-d)+\phi] \quad -d \leq x \geq d \tag{26}$$

$$E_y^{(2)}(x) = Asech[\gamma(x+d)+\psi_2] \quad x \leq d \tag{27}$$

Eqn. 26 describes the solution for the linear core region of thickness $2d$, with $d = 5\mu m$. The parameters are given as:

$$\begin{aligned} &B = 5.0 \times 10^5 \ (TE0,\ TE1,\ TE2\ modes) \\ &\lambda = 1.55\mu m \\ &\alpha = 2.44 \times 10^{-12}\ (V/m)^{-2} \\ &\epsilon_1 = 2.403 \\ &\phi = 1.5\ (TE1\ mode),\ 0.\ (TE0\ and\ TE2\ modes) \end{aligned} \tag{28}$$

The constant, K is evaluated as

$$K^2 = \epsilon_1 k^2 - \beta^2 \tag{29}$$

where k is the wave number and β is the propagation constant.

The two nonlinear cladding regions, represented by Eqns. 25 and 27, are symmetric which would allow for the simplification of the constants and other variables.

$$\begin{aligned} &A = 5. \times 10^5\ (TE0\ and\ TE1\ modes),\ \ -5.75 \times 10^5\ (TE2\ mode) \\ &\epsilon = 2.253 \\ &\psi_0,\ \psi_2 = cosh^{-1}(A/E^{(0)}),\ cosh^{-1}(A/E^{(2)}) \end{aligned} \tag{30}$$

The constant γ can be evaluated by

$$-\gamma^2 = \epsilon k^2 - \beta^2 \tag{31}$$

The other constants in Eqns. 25 and 27 are determined in a similar way as the linear equation. This set of exact solution is fully nonlinear but smooth with no numerical and physical instabilities present for a range of A and B constants from $500\ V/m$ up to $5 \times 10^5\ V/m$.

5 Discussion of Results

To verify our algorithm we compared the exact solution presented previously with the computed solutions. A two-dimensional hexahedral mesh is generated using Truegrid[6], a commercial grid generation package. This mesh consists

of 32,200 elements, 49,068 nodes, 130,077 edges and 113,210 faces. This mesh configuration was chosen as a result of several mesh refinement and redistribution work. This was necessary in order to ensure that we can properly resolve the optical wave as it propagates through the fiber. The computational domain was chosen such that the waves in the cladding was fully decayed at the outer boundaries of the cladding and the propagation direction was chosen long enough to be able to make the comparisons. The core material is glass and the two identical nonlinear claddings is nitrobenzene. Sommerfeld boundary condition is enforced at the exit and PEC (perfect electric conductor) conditions are enforced everywhere else.

The simulation is started when the input optical wave is launched at the inlet $y = 0$. The continuous wave voltage source has a spatial dependence shown in Eqns. 25-26 while the temporal dependence is a continuous sine wave. The leading-edge of the wave front is characterized by a Gaussian envelope and reaches a full sine wave at the end of its rise time. The optical wave is allowed to propagate through the core for about 10μ. Snapshots of the computed electric field magnitude, E at $t = 2.52 \times 10^{-9}s$ and $t = 7.10 \times 10^{-9}s$ are shown in Figs. 3-5 for all the TE modes. The color contours has a range of $5.2 \times 10^5 V(red)$ down to $0.0V(blue)$. The leading edge of the wave front is charaterized by the Gaussian envelope which is not used in the analytical solution. Comparison between the computed and exact solutions are made when this Gaussian envelope has passed through the fiber. The propagation of the optical waves remain smooth throughout the rest of the simulation time.

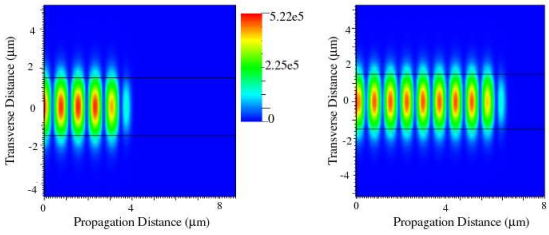

Fig. 3. TE0 mode propagation at $t = 2.52 \times 10^{-9}$ and at $t = 7.10 \times 10^{-9}s$.

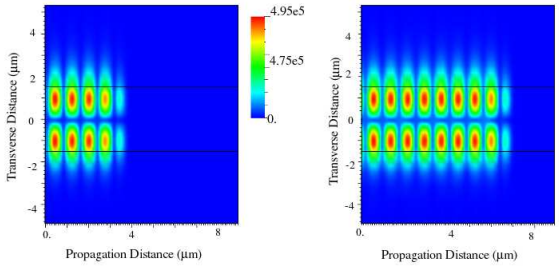

Fig. 4. TE1 mode propagation at $t = 2.52 \times 10^{-9}$ and at $t = 7.10 \times 10^{-9}s$.

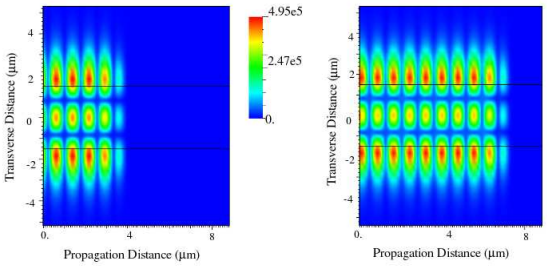

Fig. 5. TE2 mode propagation at $t = 2.52 \times 10^{-9}$ and at $t = 7.10 \times 10^{-9} s$.

In Fig. 6 lineplot comparisons between TE0 computed and analytical solutions are shown at $x = 0$ and as a function of the propagation distance. Good comparison is obtained with the maximum error (percent difference between the exact and computed solution) to be less than 5 %. Further comparisons between exact and computed solutions are presented in Figs. 7-9 at a propagation distance of $y = 3\mu m$ and at $t = 7.10 \times 10^{-9} s$. Differences in the comparisons are observed in the areas of high gradients.

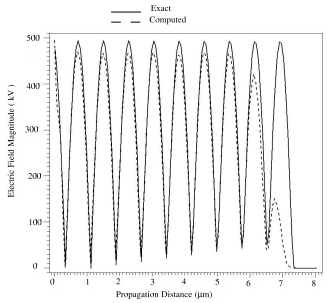

Fig. 6. TE0 mode comparison between exact and computed solution at $t = 7.10 \times 10^{-9} s$.

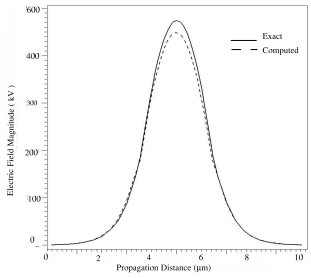

Fig. 7. TE0 mode comparison between exact and computed solution at $t = 7.10 \times 10^{-9} s$ and $y = 3\mu m$.

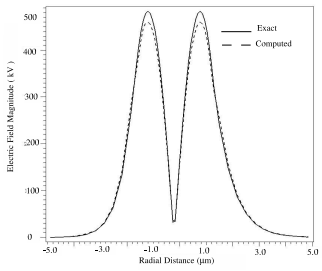

Fig. 8. TE1 mode comparison between exact and computed solution at $t = 7.10 \times 10^{-9}s$ and $y = 3\mu m$.

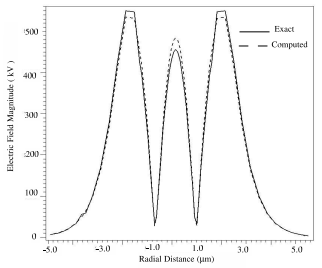

Fig. 9. TE2 mode comparison between exact and computed solution at $t = 7.10 \times 10^{-9}s$ and $y = 3\mu m$.

The second simulation we performed is that of a fully three-dimensional time-dependent simulation of an optical fiber. In practice, this usually requires a larger domain than considered here. However, just to verify our algorithm a much smaller domain is considered. The hexahedral mesh consists of 62,013 nodes, 58,320 elements, 182,288 edges, and 178,596 faces. The optical fiber has a core radius of 1.5 μm, and a cladding radius of 4.0 μm with a propagation distance of about $3\mu m$. The purpose of this simulation is to verify our algorithm for a more realistic computational domain and to increase the intensity of the input wave such that other non-linear effects might be observed. The input wave launched at the inlet section is a three-dimensional version of the exact solution presented in Eqns. 25-27 for a TE0 mode case. Here, $B = 5 \times 10^5$ and $A = 2.5 \times 10^5$. The temporal dependence is prescribed as a continuous sine wave with a Gaussian envelope at the leading edge of the wave. The input wave is propagated for up to $t = 0.671 \times 10^{-9}s$. he time evolution of the weakly guided wave, Fig. 10, is presented for $t = 0.229 \times 10^{-9}s$,$t = 0.389 \times 10^{-9}s$, and for $t = 0.459 \times 10^{-9}s$ at a given z-station of $0.9\mu m$. The maximum value of the electric field is set at their individual levels in Figs. 10a-c in order to see the details of the wave deformation. The peak value for Fig. 10a is $2.3 \times 10^6 V$ (red), Fig. 10b is $10.7 \times 10^6 V$(green), and Fig. 10c is $18.8 \times 10^6 V$(light blue). Notice that the wave starts to spread out and steepen as it evolves in time. This trend can be readily seen in Fig. 10d, where a lineplot comparison at the transverse location of $y = 0\mu m$ is plotted starting at $t = 0.229 \times 10^{-9}s$ (blue) to $t = 0.459 \times 10^{-9}s$ (grey).

The spatial progression for a fixed time, $t = 0.459 \times 10^{-9}s$ is presented next in Fig. 11 for $z = 0.48\mu m$, $z = 1.80\mu m$, and $z = 2.25\mu m$. As the pulse travels in the propagation distance, the shape and magnitude of the pulse also changes. Polarization effect is also noticed in the latter two stations. The maximum range of the electric field is $17.0 \times 10^6 V$ (red) for all three slices. In the last sub-figure (Fig 11d), a lineplot comparison at $y = 0\mu m$ is plotted for $z = 0.48\mu m$ (blue) up to $z = 2.25\mu m$ (grey), to show other details of the wave.

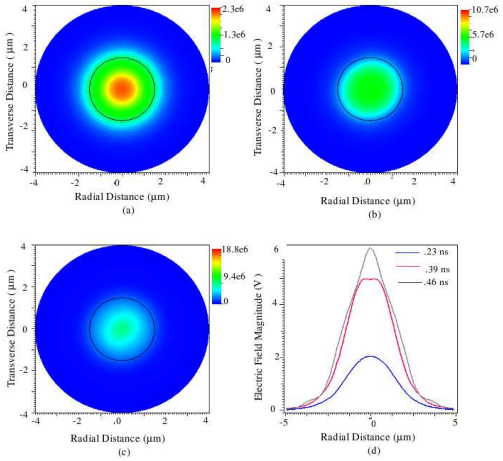

Fig. 10. TE0 mode temporal evolution in a cylindrical waveguide, (a) $t = 0.229 \times 10^{-9}$ s, (b) $t = 0.389 \times 10^{-9}$ s, (c) $t = 0.459 \times 10^{-9}$ s, (d) Line plot comparison at $y = 0\mu m$.

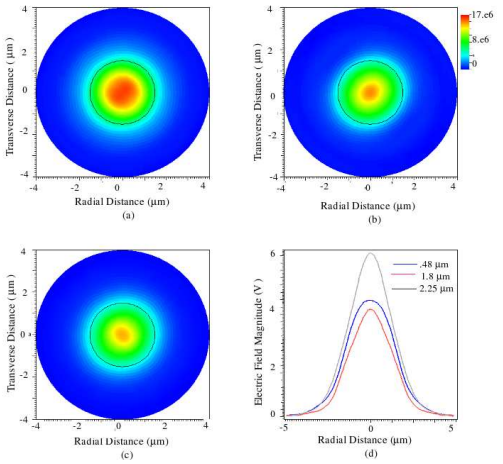

Fig. 11. TE0 mode spatial propagation in a cylindrical waveguide, (a) $z = 0.48\mu m$, (b) $z = 1.80\mu m$, (c) $z = 2.25\mu m$, (d) Line plot comparison at $y = 0\mu m$.

6 Concluding Remarks

A perturbation approach to solve a nonlinear Maxwell's equation due to Kerr effect was presented and discussed. This approach simplifies the nonlinear equations into two linear equations that can be solved numerically using Vector Finite Element formulation. To validate our approach, an exact nonlinear soution was propagated in time and space and compared with the computed solution. Good agreement was obtained between the exact and computed solution for an electric field input of medium intensity. The second simulation we performed was propagating an optical wave in a short fiber for a highly intense electric field input. Reshaping of the wave both in time and space are observed. Polarization effects are also noticed. In the next paper, further studies will be done to quantify the balancing effects between nonlinearity and dispersion.

References

[1] Nedelec, J. C. "Mixed Finite Elements in R3", *Numer. Math.*, vol 35, pp. 315-331, 1980.

[2] G.Rodrigue and D. White "A vector finite element time-domain method for solving Maxwell's equations on unstructured hexahedral grid", *SIAM J. Sci. Comp*, vol 23, pp. 683-706, 2001.

[3] K. IIzuka,*Elements of Photonics, Vol II, For Fiber and Integrated Optics* , Editor: B. Saleh, Boston University John Wiley & Sons, 2002.

[4] M. Mansuripur, *Classical Optics and its Applications*, 3rd ed. Cambridge University Press, 2002.

[5] G. Agrawal *Nonlinear Fiber Optics*, 3rd ed. Academic Press, 2001.

[6] XYZ Scientific Applications Inc, "TrueGrid home page", *http://www.xyz.com*, 2002.